Yañez et al., [MEPS]

Relative importance of predatory vs. non-predatory mortality for dominant copepod species in the northern Chile (23ºS) Humboldt Current Ecosystem

Sonia Yáñez[1,2], Pamela Hidalgo[2] and Kam W. Tang[3]

1. Doctoral Program in Oceanography, Department of Oceanography, Faculty of Natural Science and Oceanography, University of Concepcion, P.O. Box 160 C, Concepción, Chile

2. Department of Oceanography and Millennium Institute of Oceanography, Faculty of Natural Science and Oceanography, University of Concepcion, P.O. Box 160 C, Concepción, Chile.

3. Department of Biosciences, Swansea University, Swansea, SA2 8PP, U.K.

Corresponding author: P. Hidalgo (pahidalg@udec.cl)

Short title: Copepod mortalities in Chilean Humboldt Current

Abstract

Copepods dominate the zooplankton communities and support large fisheries within the Humboldt Current System (HCS). Using detailed data of live/dead compositions, along with stage durations and molting rates, we derived for the first time both predatory and non-predatory mortality rates of the three main copepod species, *Paracalanus* cf. *indicus*, *Acartia tonsa* and *Calanus chilensis*, within HCS, and examined their relations with environmental factors. Predatory mortality rates of all three species increased linearly with developmental stages, hence body sizes, indicating top-down control by predators that prefer larger prey. Intrusion of oxygen-poor water via upwelling and low chlorophyll *a* concentration were linked to increased non-predatory mortality rates of *P. cf. indicus* and *A. tonsa*, whereas non-predatory mortality rate of *C. chilensis* was positively correlated with temperature. On average, non-predatory mortality accounted for 34.8 to 46.3 % of the total mortality among the three species. Changes in upwelling intensity caused by climate change may alter the extents and patterns of predatory and non-predatory mortalities in the HCS copepod communities.

Keywords: Copepods mortality, Neutral Red stain, copepod carcasses, Vertical Life Table, Chilean Humboldt Current System.

1. Introduction

Mortality is a critical but poorly quantified parameter in copepod population dynamics (Ohman & Wood 1995, Runge et al. 2004). The main cause of copepod mortality is generally assumed to be predation (Verity & Smetacek 1996), but many non-predatory factors can also cause mortality, such as diseases (Delgado & Alcaraz 1999), parasites (Kimmerer & McKinnon 1989, Burns 1985, Ohtsuka et al. 2004), physical and chemical stresses (Roman et al. 1993; Bickel et al. 2011), starvation (Tsuda 1994), and senescence (Ceballos & Kiørboe 2011; Saiz et al. 2015), all of which may leave carcasses behind. Indeed, a meta-analysis of literature data suggests that up to one-third of the mortality in marine pelagic copepods can be attributed to non-predatory causes (Hirst & Kiørboe 2002), and copepod carcasses have been observed around the world, at times in high abundances (Yañez et al. 2012; Tang et al. 2014; Yañez et al. 2018; Tang et al. 2019b).

Recent studies have shown that ignoring even a small magnitude of carcass abundance and non-predation mortality could lead to large errors in population growth and secondary production estimates (Elliott and Tang 2011a; Yañez et al. 2018). Furthermore, predatory mortality represents an upward trophic transfer of copepod biomass, whereas non-predatory mortality represents a potential diversion of copepod production to the microbial loop (Tang et al. 2006, 2009; Bickel & Tang 2010) or sinking fluxes (Sampei et al. 2009, 2012; Ivory et al. 2014; Tang et al. 2019a). Therefore, proper quantification and separation of predatory and non-predatory components of mortality is critical to a more accurate understanding of the pelagic food web. In this regard, the Neutral Red staining method allows researchers to distinguish between live and dead zooplankton in field samples (Elliott & Tang 2009), thereby providing a means to quantify predatory and non-predatory mortalities (Elliott &Tang 2011a; Yañez et al. 2012, 2018).

The Humboldt Current System (HCS) is among the most productive pelagic ecosystems (Thiel et al. 2007). Copepods dominate its zooplankton communities and support large fisheries

77 in the region (Espinoza & Bertrand 2008). Copepod population abundances within the HCS can
78 be highly variable (Hidalgo et al. 2010, 2012; Pino-Pinuer 2014), but investigation of copepod
79 mortality rates and patterns has been lacking. In northern Chile, Mejillones Bay (23°S) is one of
80 the most important upwelling centers within the HCS (Marín et al. 1993). Shallow cold-water
81 masses with low oxygen concentration (Equatorial Subsurface Water, ESSW) associated with the
82 Oxygen Minimum Zone (OMZ) are present due to upwelling events that occur year-round
83 (Marín & Olivares 1999). The ESSW supports a high zooplankton diversity, with at least 107
84 species of copepods (Hidalgo et al. 2010), nine of which are numerically dominant (Escribano et
85 al. 2012). The abundance and biomass of the copepod community in Mejillones Bay are
86 influenced by the vertical distribution of dissolved oxygen (Yañez et al. 2012), upwelling
87 intensity (Escribano et al. 2009, 2012), upwelling shadow and advection (Giraldo et al. 2002). A
88 recent study suggests that the copepods are highly sensitive to environmental variability, as
89 reflected by changing abundance of copepod carcasses in the coastal waters in response to
90 changes in upwelling intensity that reduce or expand the oxygenated surface layer in HCS
91 (Yañez et al. 2012).

92 In this study, we used the Neutral Red staining method to measure the stage-specific live/dead
93 compositions of the three major copepod species: *Calanus chilensis*, *Acartia tonsa* and
94 *Paracalanus* cf *indicus* in the Mejillones Bay (Hidalgo & Escribano 2001, Hidalgo et al. 2010)
95 over two annual cycles. From these data we then, for the first time, calculated and compared
96 their predatory and non-predatory mortality rates, and examined their relationships with the
97 environmental conditions.

98 **2. Materials and Methods**

99 **2.1 Field sampling**

100 The study was conducted in northern Chile (Mejillones Bay) within the Humboldt Current
101 System (HCS). Monthly sampling was performed from January of 2010 to December of 2011 at

three stations along a coastal transect: St-1 (23º 04.2'S, 70º 25.8'W; maximum station depth (z_{max}) = 60 m), St-2 (23º 02.4'S, 70º 27.0'W; z_{max} = 90 m) and St-3 (23º 0.2'S, 70º 28.2'W; z_{max} = 120 m) (Fig.1). Water temperature, salinity, and dissolved oxygen (DO) were measured at each station using an autonomous oceanographic profiler CTD-O SeaBird SBE-19 plus deployed down to 50-m depth. Phytoplankton biomass was measured as concentrations of chlorophyll *a* (Chl-*a*). Water samples for Chl-*a* measurements (at 10 and 50 m depths) were obtained using a 5-L Niskin bottle. Chl-*a* was measured fluorometrically after filtration onto GF/F (0.7 mm) filters (Morales & Anabalon 2012; Anabalon et al. 2014). Intensity of upwelling was calculated as Ekman transport using the equation of Mann & Lazier (1991):

$$M_x = \frac{\tau y}{f} \quad [1]$$

where M_x is Ekman transport ($m^3\ s^{-1}\ km^{-1}$), f is the Coriolis parameter and τ_y is along-shore wind stress (ρ_a). M_x is positive for south wind (upwelling) and negative for north winds (downwelling). τ_y was estimated as:

$$\tau_y = \rho_a \times Cd \times (V_y|V_y|) \quad [2]$$

where ρ_a is air density (1.21 kg m^{-3}), Cd is the empirical constant of drag coefficient (=0.0014), and V_y is the along-shore wind velocity (m s^{-1}). Ekman transport was averaged monthly from daily estimates based on wind data from the meteorological station in Cerro Moreno airport (http://164.77.222.61/climatologia/)

Copepods were collected by vertical hauls through 0−30 m during the day using a WP-2 net (200 µm mesh and a 50-cm mouth diameter) equipped with a flowmeter. The abundance data were corrected for potential undersampling according to Yañez et al. (2018). We applied the correction factors only for C1–C3 of *Acartia tonsa* and *Paracalanus* cf. *indicus*, and C1 and C2 of *Calanus chilensis* because there were no differences between mesh sizes for the later stages. Our target copepod species are concentrated in this oxygenated upper layer (Hidalgo et al. 2010; Yañez et al. 2012; Donoso & Escribano 2014; Ruz et al. 2015). Upon retrieval of the net, the

samples were transferred to a chilled container and immediately treated with the vital stain Neutral Red (Elliott & Tang 2009, modified by Yanez 2009 and Yanez et al. 2012 for local conditions). Briefly, each sample was incubated with 2−4 ml of Neutral Red stock solution (0.5% w/v) for 10 min. Afterward, the stained samples were concentrated and briefly rinsed with filtered seawater to remove excess stain, then preserved in 4% neutralized formalin solution in the dark, and processed further in the laboratory within 3−6 months. In the laboratory, the stained samples were concentrated and briefly rinsed with filtered seawater, then acidified by 0.3 ml of 1M acetic acid to develop the stain's color. Under a stereo-microscope (20–40 ×), the dominant copepod species *Paracalanus* cf. *indicus*, *Acartia tonsa* and *Calanus chilensis* were counted and identified to developmental stages from entire samples. The body size was measured using a calibrated reticule (micro-ruler) attached to the eyepiece of the microscope. Individuals that were alive at the time of sampling appeared red, whereas dead ones remained unstained.

2.2 Copepod stage durations

Development times of the different stages were calculated from empirically measured molting rates (Equations 2 and 3 in Table S1). Details of the molting rate experiments are reported in Yañez et al. (2018). The data were then applied to equation of Beléhrádek (1935) (Equation 1 in Table S1) for the relevant environmental temperatures (Table S2) to derive *in situ* stage-specific development times; these development times were used to calculate stage durations (D_i for stage i, days), which were then used to calculate mortality rates.

All three copepod species showed significant temporal and ontogenetic differences in stage durations (Fig. S1; Table S3). Stage durations decreased with increasing temperature in all three species. For *P. cf. indicus* and *C. chilensis*, development progressed with similar stage durations through the early copepodite stages (C1–C3), then slowed through the C4 and C5 stages (i.e. longer stage durations). For *A. tonsa*, development progression was almost identical between C1 and C2, and between C3 and C4, then slowed considerably in C5. Overall, *A. tonsa* tended to

152 have shorter stage durations than the other two species for all stages and across all temperatures.
153
154 **2.3 Predatory and non-predatory mortality rates**

155 We estimated the predatory and non-predatory components of mortality using the Vertical Life
156 Table (VLT) method as modified by Elliott & Tang (2011a) by distinguishing between live
157 copepods and carcasses (Table S1). In this method, both live copepods and intact carcasses were
158 treated as survivors of predation, but only live individuals proceeded to the next life stages.
159 Thus, by using both the abundances of live copepods and carcasses, stage duration and carcass
160 turnover rates (Equation 4 in Table S1), predatory mortality rate and total mortality rates were
161 solved for iteratively (Equations 5, 6 and 7 in Table S1). Non-predatory mortality was then
162 calculated as the difference between total mortality rate and predatory mortality rate.
163
164 **2.4 Statistics**

165 Normality was tested by the Kolmogorov-Smirnov test (Zar 1984). When necessary, the data
166 were log transformed (n+1) to meet the requirement of normal distribution. Seasonal and annual
167 differences in the oceanographic conditions, differences in stage duration and predatory and non-
168 predatory mortality rates among development stages and between years were tested with a two-
169 factor General Linear Model (GLM) ($\alpha = 0.05$) after checking that the data met the parametric
170 assumptions. Spearman rank correlations were used to test for linear relationships between
171 parameters ($\alpha = 0.05$). Statistical analysis was done using Minitab v. 11.
172
173 **3. Results**
174 **3.1 General oceanographic conditions**
175 Oceanographic conditions for both years are summarized in Table S2. The Ekman transport
176 was positive during much of the study period, indicating prevailing upwelling conditions (Fig.

177 2a). In contrary to the previous suggestion of weak seasonality of upwelling in Mejillones Bay
178 (Sobarzo et al. 2007), we observed significant seasonal variations in Ekman transport (Table S3),
179 with the strongest Ekman transport occurring in late winter and early spring, reaching 700 m^3 s^{-1}
180 km^{-1} in October 2010 and 941 m^3 s^{-1} km^{-1} in September 2011, whereas the lowest values were
181 found in the fall. Water column temperature ranged between 11.9 °C and 17.3 °C during the
182 sampling period. A warmer period in the summer/fall and a colder period of winter/spring
183 months (Fig. 2b). The water column was strongly thermally stratified, with the isotherm of 16 °C
184 at 10 m depth most of the time. The lowest temperatures were recorded in water deeper than 50
185 m. Intrusion of cold upwelled water caused the shoaling of the 14 °C isotherm to near 20 m
186 between July 2010 and March 2011 and in September 2011.
187 Salinity was rather stable at 34.8–34.9 in both years (Fig. 2c) and without significant changes
188 between seasons (Table S3). Dissolved oxygen concentration showed similar seasonal patterns
189 between years, with an oxycline at 10–20 m depth (Fig. 2d). In 2010, the average upper
190 boundary of the OMZ (1 ml O_2 l^{-1}) was at 22.0 ± 8.8 m and a very deep OMZ was observed in
191 August. In 2011, the upper limit of the OMZ was at an average depth of 26.0 ± 17.0 m and was
192 deeper than in the previous year between June and September. Chlorophyll *a* concentrations
193 showed significant seasonal and yearly differences (Fig. 2e, Table S3).
194
195 **3.3 Predatory and non-predatory mortality rates**
196 There were significant ontogenetic and temporal differences in predatory mortality rate
197 among the three copepod species (Table S5). The estimated predatory mortality rate of *P.* cf.
198 *indicus* was generally higher in the older stages of C3–C5 than in the younger stages of C1–C2
199 in both years (Fig. 3 a,b). The predatory mortality rate of *A. tonsa* reached its highest value in
200 C2–C5, especially in the winter-spring period (September–December) in both years, and lowest
201 in the summer period (January–March) (Fig. 3 c,d). Likewise, the predatory mortality rate of *C.*

202 *chilensis* was lowest in the summer and fall, and was very high in stages C2–C5, especially in
203 November (Fig 3 d, e). Predatory mortality was positively correlated with dissolved oxygen for
204 all three species, negatively with chlorophyll *a* for *A. tonsa*, and negatively with temperature for
205 *C. chilensis* (Table S5).

206 There were significant ontogenetic, but not temporal, differences in non-predatory mortality
207 rate of *P.* cf. *indicus* and *C. chilensis*, and the rate also varied significantly between months in *A.*
208 *tonsa* (Table S5). The estimated non-predatory mortality rate of *P.* cf. *indicus* was generally
209 higher in stage C5 in 2011, and lower in C1–C2 in both years (Fig. 4 a,b). The non-predatory
210 mortality rate of *A. tonsa* was highest in C1–C4 in the spring (September–December) in both
211 years and in C5 in the fall–winter period (April–July), and lowest in the summer period
212 (January–March) (Fig. 4 c,d). Likewise, the non-predatory mortality rate of *C. chilensis* was
213 lowest in the summer, and was high in the spring especially for C5 (Fig. 4 d, e). Non-predatory
214 mortality was significantly and negatively correlated with dissolved oxygen and chlorophyll *a* in
215 both *P.* cf. *indicus* and *A. tonsa*, whereas it was positively correlated with temperature in *C.*
216 *chilensis* (Table 1).

217 Total mortality rates over the two years increased with developmental stages in all three
218 species (Table 2, Fig. 5). The partition of mortality between predatory and non-predatory
219 sources, however, remained rather constant across the developmental stages for each species,
220 with predation contributing to a larger portion of the total mortality. On average, predation
221 accounted for 53.7% of the total mortality in *P. cf. indicus*, 56.4% in *A. tonsa*, and up to 65.2%
222 in *C. chilensis* (Table 2, Fig. 5).

223

224 **4. Discussion**

225 The high variability of copepod abundances within the HCS (Hidalgo et al. 2010, 2012; Pino-

Pinuer 2014; Yañez et al., 2018) suggests a very dynamic balance between birth and mortality. In addition to predation, the presence of OMZ and upwelling events are also key drivers of population dynamics and secondary production within the HCS (Escribano et al. 2009, 2012; Yañez et al. 2012). During this study, the chlorophyll *a* concentration was variable, but it was generally at levels not considered to be limiting to zooplankton (Escribano et al. 2016), except in the winter months when the water column was more mixed and the OMZ was restricted to the deeper depths, and when chlorophyll *a* was nearly depleted (0.02 mg m^{-3}). The water column was thermally stratified with low DO for much of the years, consistent with previous findings (Escribano et al. 2004; Ruz et al. 2015, 2017).

An interesting observation from this study is that mortality rate increased with developmental stages in all three species. Elliott & Tang (2011a) showed that over an annual cycle in the Chesapeake Bay, copepodite mortality rates were generally higher than naupliar mortality rates. In Lurefjorden, Norway, where predatory copepods were abundant, the mortality rate of *Calanus* spp. decreased substantially as the copepod developed through the naupliar stages, but subsequently increased slightly between C1 and CV (Eiane et al. 2002). A similar increase in mortality rate in late copepodite stages was also observed in *Calanus finmarchicus* in the North Sea (Eiane & Ohman 2004).

In our study, we observed that the older copepod stages had longer stage duration than the younger stages (Fig. S1), which agrees with an earlier study (Escribano et al. 1998). The increasing stage duration means an increasing chance for the older stages to succumb to both predatory and non-predatory mortalities. The estimated mortality rates of C1 were comparable to the global average values (ca. 0.10–0.15 d^{-1}; Hirst & Kiørboe 2002) for the observed temperature range, but were much higher for the later stages (up to 0.55 d^{-1}). Nevertheless, similarly high CV-adult mortality rates have been reported elsewhere; for example, a mortality of ca. 0.5 d^{-1} has been reported by Ohman & Hsieh (2008) for *Calanus pacificus* within the California coastal

upwelling system, and by Maud et al. (2018) for *Calanus helgolandicus* at L4 station. Elliott & Tang (2011) derived temperature-dependent copepodite mortality for *Acartia tonsa* in the Chesapeake Bay, reaching ca. 0.5 d^{-1} at 14 °C, which is nearly the same as our estimate for that average water temperature.

Apparently, these copepod species have different strategies to maintain their populations despite the high estimated mortality rates. The spawning frequency of these species is unknown, but is probably high because all life stages can be found year-round (Escribano et al. 2007; Hidalgo & Escribano 2008; Ruz et al. 2015), indicating frequent reproduction and short life cycles. A fast Development Rates (DR) may allow young stages to reach maturity sooner, thereby ensure a continuous supply of gravid females. For example, *Calanus chilensis* development time is 22 days at 17°C (Escribano et al., 1998), with 17 generations per year; *Paracalanus* cf. *indicus* development is 8 days at 17°C, with 45 generations per year (Escribano et al., 2014), while *Acartia tonsa* is 25 days at 17°C (McLaren et al., 1969), with 15 generations per year. Moreover, *C. chilensis* has been shown to have high egg production rate (EP; 29 eggs $female^{-1}$ d^{-1}) (Escribano et al., 2014), whereas *P.* cf. *indicus* and *A. tonsa* have high egg hatching success (HS; 52% and 73%, respectively) (Escribano et al., 2014; Ruz et al.,2015). Therefore, fast DR coupled with high HS in *P.* cf. *indicus* and *A.tonsa* and high EP in *C.chilensis* appear to be their strategies for sustaining their populations and achieving dominance in the HCS.

Using Neutral Red staining and the modified VLT method, we were able to partition mortality into predatory and non-predatory sources. Predatory mortality rates of all three species increased linearly with developmental stages, hence body sizes. Larger body sizes may make the copepodites more conspicuous to visual predators such as planktivorous fish, which often prefer the larger prey (Brooks 1968; O'Brien et al. 1976). Within the HCS, the major planktivores include sardines and anchovies in the oxygenated layer (Espinoza & Bertrand 2008), which may

explain the observed positive relationship of predatory mortality rates with the copepodite stage (i.e. body size), as well as with DO in two of the three species.

Intermittent intrusion of oxygen-poor water associated with coastal upwelling is a common feature in the region (Marín et al. 1993), which could cause episodic hypoxia and copepod mortality (Elliott et al. 2010; Yañez et al. 2012; Elliott et al. 2013). In our study, low DO was associated with high non-predatory mortality rates of *P.* cf. *indicus* and *A. tonsa*, consistent with earlier reports (Yáñez et al. 2012; Ruz et al. 2015). In contrast, low DO did not have a significant effect on *C. chilensis*, reflecting the latter species' better ability to cope with low oxygen environment (Hirche et al. 2014; Ruz et al. 2018).

Non-predatory mortality rates of *P.* cf. *indicus* and *A. tonsa* were negatively correlated with chlorophyll *a* concentration, implying direct or indirect food limitation effects. Interestingly, temperature correlated positively with non-predatory mortality rate, but negatively with predatory mortality rate of *C. chilensis*. This species is endemic to the coastal upwelling system (Escribano & Rodriguez 1994, 1995; Escribano 1998; Torres & Escribano 2003). Increasing water column temperature reflects the weakening of the upwelling condition, which may lead to a less favorable living condition and thence a higher non-predatory mortality rate. Meanwhile, a less stratified condition may allow the copepod to migrate deeper diurnally to avoid predation (Hidalgo et al. 2005), resulting in a lower predatory mortality rate.

Overall, the relative proportions of predatory vs. non-predatory mortality rates remain fairly consistent across developmental stages within a species. On average, non-predatory mortality accounts for 34.8 to 46.3 % of the total mortality. This highlights the importance of non-predatory factors such as environmental stresses in driving copepod population dynamics within HCS (Escribano et al. 2012; Pino-Pinuer et al. 2014; Medellin-Mora 2016).

5. Conclusions

We investigated copepod mortality rates within HCS, and examined the relative importance of predatory and non-predatory mortalities in relation to environmental conditions. In the Southwest Pacific, climate change is expected to intensify upwelling in HCS (Echevin et al. 2012). In such a scenario, stronger upwelling may promote extreme shoaling of the OMZ, which compresses the habitat range for zooplankton (Manríquez et al. 2009), and which will likely alter the extents and patterns of both predatory and non-predatory mortality rates of the copepod populations. It is therefore pertinent that researchers consider both mortality sources in order to fully understand copepod population dynamics within this important ecosystem.

Acknowledgements

This work was supported by the CONICYT-FONDECYT No. 11090146 and No. 1191343 (P. Hidalgo) 1181682 (P. Hidalgo and R. Escribano) and International cooperation CONICYT project: RED180141.Yañez was supported by the Scholarship of CONICYT-PCHA/Doctorado Nacional/2013-21130213 and by Red Doctoral en Ciencia, Tecnología y Ambiente, REDOC CTA, University of Concepcion. The authors thank Dr. David Elliott and Benjamin Glasner for helping with data analysis, Captain Juan Menares and the crew of R/V Menachos for assistance in the field. This work is a contribution by International Collaboration Program REDES No 180141 and Millennium Institute of Oceanography ICM 120019.

References

Anabalón V, Arísteguia J, Morales CE, Andrade I, Benavides M, Correa-Ramírez MA, Espino M, Ettahiri O, Hormazabal S, Makaoui A, Montero MF, Orbi A (2014) The structure of planktonic communities under variable coastal upwelling conditions off Cape Ghir (31°N) in the Canary Current System (NW Africa). Prog Oceanogr 120:320–339.

325 Beléhrádek J (1935). Temperature and living matter. Protoplasma Monogr. 8:1–277.

326 Bertrand A, Ballón M, Chaigneau A (2010) Acoustic observation of living
327 organisms reveals the upper limit of the oxygen minimum zone. PLoS One 5, e10330.

328 Bickel S, Tang K (2010) Microbial decomposition of proteins and lipids in copepod versus
329 rotifer carcasses. Mar Biol 157:1613–1624.

330 Bickel SL, Hammond JDM, Tang KW (2011) Boat-generated turbulence as a potential source of
331 mortality among copepods. J Exp Mar Biol Ecol 401:105–109.

332 Brooks LJ (1968). The effects of prey size selection by lake planktivores. Systematic Biology
333 17(3): 273–291.

334 Burns CW (1985) Fungal parasitism in a copepod population: the effects of Aphanomyces on the
335 population dynamics of *Boeckella dilatata* Sars. J Plankton Res 7: 201–205.

336 Ceballos S, Kiørboe T (2011) Senescence and sexual selection in a pelagic copepod. PLoS One
337 6(4):18870. doi:10.1371/journal. pone.0018870.

338 Daneri G, Dellarossa V, Quiñonez R, Jacob B, Montero P, Ulloa O (2000) Primary production
339 and community respiration in the Humboldt Current System off Chile and associated oceanic
340 areas. Mar Ecol Prog Ser 97: 41–49.

341 Delgado M, Alcaraz M (1999) Interactions between red tide microalgae and herbivorous
342 zooplankton: the noxious effects of *Gyrodinium corsicum* (Dinophyceae) on *Acartia grani*
343 (Copepoda: Calanoida). J Plankton Res 21: 2361–2371.

344 Donoso K, Escribano R (2014) Mass-specific respiration of mesozooplankton and its role in the
345 maintenance of an oxygen-deficient ecological barrier (BEDOX) in the upwelling zone off Chile
346 upon presence of a shallow oxygen minimum zone. J Mar Syst 129: 166-177.

347 Dorazio RM (1984) The contribution of longevity to population death rates. Hydrobiologia
348 108:239–243.

349 Echevin V, Goubanova K, Belmadani A, Dewitte B (2012) Sensitivity of the Humboldt Current
350 system to global warming: a downscaling experiment of the IPSL-CM4 model. Climate Dynam
351 38: 761–774.

352 Eiane K, Aksnes DL, Ohman MD, Wood S, Martinussen MB (2002) Stage-specific mortality of
353 Calanus spp. under different predation regimes. Limnol. Oceanogr 47:636-645.

354 Eiane K, Ohman MD (2004) Stage-specific mortality of *Calanus finmarchicus*, *Pseudocalanus*
355 *elongates* and *Oithona similis* on Fladen Ground, North Sea, during a spring bloom. Mar Ecol
356 Prog Ser 268:183-193.

357 Elliott DT, Tang KW (2009) Simple staining method for differentiating live and dead marine
358 zooplankton in field samples. Limnol Oceanogr Methods 7: 585–594.

359 Elliott DT, Harris CK, Tang KW (2010). Dead in the water: The fate of copepod carcasses in the
360 York River estuary, Virginia. Limnol Oceanogr 55: 1821–1834.

361 Elliott DT, Tang KW (2011a). Influence of carcass abundance on estimates of mortality and
362 assessment of population dynamics in *Acartia tonsa*. Mar Ecol Prog Ser 427: 1–12.

363 Elliott DT, Tang KW (2011b) Spatial and temporal distributions of live and dead copepods in the
364 lower Chesapeake Bay (Virginia, USA). Estuar Coasts 34: 1039–1048.

365 Elliott DT, Pierson JJ, Roman M (2013) Copepods and hypoxia in Chesapeake Bay: abundance,
366 vertical position and non-predatory mortality. J Plankton Res 35: 1027–1034.

Escribano R and Rodriguez L (1994). Life cycle of Calanus chilensis Brodsky in northern Chile. In: Ecology and Morphology of Copepods. F.D. Ferrari & B.P. Bradley (eds). Kluwer Academic Publishers, Boston. pp. 289-294.

Escribano R, Rodriguez L (1995) Seasonal size variation and growth of *Calanus chilensis* Brodsky in northern Chile. Revista Chilena de Historia Natural. 68: 373-382.

Escribano R (1998) Population dynamics of *Calanus chilensis* in the Chilean Eastern Boundary Humboldt Current. Fish Oceanogr 7(3/4): 245-251.

Escribano R, Rodríguez L and Iribarren C (1998) Temperature-dependent development and growth of Calanus chilensis Brodsky from Northern Chile. J Exp Mar Biol Ecol 229: 19-34.

Escribano R, Daneri G, Farías L, Gallardo VA, Gonzaález HE, Gutiérrez D, Lange CB, Morales, CE, Pizarro O, Ulloa O, Braun M (2004). Biological and chemical consequences of the 1997–1998 El Niño in the Chilean coastal upwelling system: a synthesis.Deep-Sea Res. Pt. II 51, 2389–2411.

Escribano R, Hidalgo P, González HE, Giesecke R, Riquelme-Bugueño R, Manríquez K(2007) Interannual and seasonal variability of metazooplancton in the Central/South upwelling region off Chile. Prog Oceanogr 75: 470-485.

Escribano R, Hidalgo P, Fuentes M, Donoso K (2012) Zooplankton time series in the coastal zone off Chile: Variation in upwelling and responses of the copepod community. Prog Oceanogr 97: 74–186.

Escribano R, Hidalgo P, Valdés V, and Frederick L (2014) Temperature effects on development and reproduction of copepods in the Humboldt Current: the advantage of rapid growth. J Plankton Res 36: 104–116.

390 Espinoza P, Bertrand A, (2008) Revisiting Peruvian anchovy (*Engraulis ringens*)
391 trophodynamics provides a new vision of the Humboldt Current system. Prog Oceanogr 79: 215–
392 227.

393 Genin A, Gal G, Haury L (1995) Copepod carcasses in the ocean. II. Near coral reefs. Mar Ecol
394 Prog Ser 123: 65–71.

395 Giraldo A, Escribano R, Marin VH (2002) Spatial distribution of Calanus chilensis off
396 Mejillones Peninsula (northern Chile): ecological consequences upon coastal upwelling. Mar
397 Ecol Prog Ser 230: 225–234.

398 Hall LW, Alden RW (1997) A review of concurrent ambient water column and sediment toxicity
399 testing in the Chesapeake Bay watershed: 1990–1994. Environ Toxicol Chem 16: 1606–1617.

400 Harris R, Wiebe P, Lenz J, Skjoldal HR, Huntley M (2000) ICES Zooplankton Methology
401 Manual. Academic Press. San Diego, USA.

402 Hays G, Richardson A, Robinson C (2005) Climate change and marine plankton. Trends Ecol
403 Evol 20: 337–344.

404 Hidalgo P, Escribano R, Morales CE (2005) Ontogenetic vertical distribution and diel migration
405 of the copepod *Eucalanus inermis* in the oxygen minimum zone off northern Chile. J Plankton
406 Res 27: 519–529.

407 Hidalgo P, Escribano R (2008) The life cycles of two coexisting copepods, *Calanus chilensis*
408 and *Centropages brachiatus*, in the upwelling zone off northern Chile (23°S). Mar Biol 155:
409 429–442.

410 Hidalgo P, Escribano R, Vergara O, Jorquera E, Donoso K, Mendoza P (2010) Patterns of
411 copepod diversity in the Chilean coastal upwelling system. Deep-Sea Res Part II 57: 2089–2097.

412 Hirche HJ, Barz K, Ayon P, Schulz J (2014) High resolution vertical distribution of the copepod
413 *Calanus chilensis* in relation to the shallow oxygen minimum zone off northern Peru using
414 LOKI, a new plankton image system. Deep Sea Res. Part I 188: 63–73.

415 Hirst AG, Kiørboe T (2002) Mortality of marine planktonic copepods: global rates and patterns.
416 Mar Ecol Prog Ser 230: 195–209.

417 Ivory JA, Tang KW, Takahashi K (2014) Use of Neutral Red in short-term sediment traps to
418 distinguish between zooplankton swimmers and carcasses. Mar Ecol Prog Ser 505:107–117.

419 Kimmerer WJ, McKinnon AD (1990) High mortality in a copepod population caused by a
420 parasitic dinoflagellate. Mar Biol 107, 449-452

421 Ohman MD, Hsieh C-H (2008) Spatial differences in mortality of Calanus pacificus within the
422 California Current System. J Plankton Res 30: 359–366.

423 Ohman MD, Wood SN (1995) The inevitability of mortality. ICES J Mar Sci 52: 517–522.

424 Pearre Jr S (1980) Feeding by Chaetognatha: the relation of prey size to predator size in several
425 species. Mar Ecol Prog Ser 3: 125–134.

426 Mann KH, Lazier JNR (1991) Dynamics of marine ecosystems: biological-physical interactions
427 in the oceans. Blackwell Scientific Publications, Oxford, United Kingdom. 394 pp.

428 Manríquez K, Escribano R, Hidalgo P (2009) The influence of coastal upwelling on
429 the mesozooplankton community structure in the coastal zone off Central/Southern Chile
430 as assessed by automated image analysis. J Plankton Res 31(9): 1075 – 1088.

431 McLaren IA, Corkett CJ, Zillioux EJ (1969). Temperature adaptations of copepod eggs

432 from the Artic to the tropics. Biol Bull 137 (3): 486–493.

433 Marín V, Rodríguez L, Vallejo L, Fuenteseca J, Oyarce E (1993) Efectos de la surgencia costera
434 sobre la productividad primaria primavera de la Bahía Mejillones de Sur (Antofagasta, Chile).
435 Rev Chil Hist Nat 66: 479–491.

436 Marín V, Olivares G (1999) Estacionalidad de la productividad primaria en Bahía Mejillones del
437 Sur (Chile): una aproximación proceso-funcional. Rev. Chil. Hist. Nat. 72, 629–641.

438 Morales CE, Lange BC (2004) Oceanographic studies in the Humboldt current system off Chile:
439 an introduction. Deep-Sea Research II. 51, 2345–2348.

440 Morales CE, Anabalon V (2012) Spatio-temporal distribution of chlorophyll *a*, picoplankton,
441 and nanoplankton during the spring upwelling season in the coastal area off Concepción, central-
442 southern Chile. Progr. Oceanogr. special volume.

443 Medellín-Mora J, Escribano R, Schneider W (2016) Community response of zooplankton to
444 oceanographic changes (2002–2012) in the central/southern upwelling system of Chile. Prog.
445 Oceanogr. 142:17–29.

446 O'Brien WJ, Slade, NA, Vinyard G L (1976) Apparent size as the determinant of prey selection
447 by bluegill sunfish (*Lepomis macrochirus*). Ecology 57(6): 1304–1310.

448 Ohtsuka S, Hora M, Suzaki T, Arikawa M, Omura G, Yamada K (2004) Morphology and host-
449 specificity of the apostome ciliate *Vampyrophrya pelagica* infecting pelagic copepods in the Seto
450 Inland Sea, Japan. Mar Ecol Prog Ser 282: 129–142.

451 Pino-Pinuer P, Escribano R, Hidalgo P, Riquelme-Bugueño R, Schneider W (2014) Copepod
452 community response to variable upwelling conditions off central-southern Chile during
453 2002−2004 and 2010−2012. Mar Ecol Progr Ser 515: 83–95.

454 Poulet SA, Escribano R, Hidalgo P, Cueff A, Wichardc T, Aguilera V, Vargas CA, Pohnert G
455 (2007) Collapse of Calanus chilensis reproduction in a marine environment with high diatom
456 concentration. J Exp Mar Bio Ecol 352: 187–199.

457 Roman MR, Gauzens AL, Rhinehart WK, White JR (1993) Effects of low oxygen waters on
458 Chesapeake Bay zooplankton. Limnol Oceanogr 38: 1603–1614.

459 Rodríguez-Graña L, Calliari D, Tiselius P, Hansen BW, Skold HM (2010) Gender-specific
460 ageing and non-Mendelian inheritance of oxidative damage in marine copepods. Mar Ecol Prog
461 Ser 401:1–13.

462 Runge JA, Franks PJS, Gentleman WC, Megrey BA, Rose KA, Werner FE, Zakardjian B (2004)
463 Diagnosis and prediction of variability in secondary production and fish recruitment processes:
464 developments in physical-biological modeling. In: Robinson AR, Brink KH (eds) The sea, Vol
465 13. Harvard University Press, Cambridge, MA, p 413–473.

466 Ruz PM, Hidalgo P, Yáñez S, Escribano R, Keister JE (2015) Egg production and hatching
467 success of Calanus chilensis and Acartia tonsa in the northern Chile upwelling zone (23°S),
468 Humboldt Current System. J Marine Syst 148: 200–212.

469 Ruz PM, Hidalgo P, Riquelme-Bugueño R, Franco-Cisterna B, Cornejo M (2017)
470 Vertical distribution of copepod eggs in the oxygen minimum zone off Mejillones Bay
471 (23°S) in the Humboldt Current System. Mar Ecol Progr Ser doi: 10.3354/meps12117

472 Ruz PM, Hidalgo P, Escribano R, Keister JE, Yebra L, Franco-Cisterna B (2018) Hypoxia
473 effects on females and early stages of Calanus chilensis in the Humboldt Current ecosystem
474 (23°S). J Exp Mar Biol Ecol 498: 61–71.

475 Saiz E, Calbet A, Grifell K, Guilherme J, Bersano F, Isari S, Solé M, Peters J, Alcaraz M (2015)
476 Ageing and caloric restriction in a marine planktonic copepod. Sci Rep 5:14962.

477 Sampei M, Sasaki H, Hattori H, Forest A, Fortier L (2009) Significant contribution of passively
478 sinking copepods to the downward export flux in Arctic waters. Limnol Oceanogr 54: 1894–
479 1900.

480 Sampei, M, Sasaki H, Forest A, Fortier L (2012). A substantial export flux of particulate organic
481 carbon linked to sinking dead copepods during winter 2007-2008 in the Amundsen Gulf
482 (southeastern Beaufort Sea, Arctic Ocean). Limnol Oceanogr 57: 90–96.

483 Sherman K (1990) Productivity, perturbations and options for biomass yield in large marine
484 ecosystems. In Sherman, K, Alexander, L.M. and Gold, B.D: (eds) Large marine ecosystems:
485 Patterns, Progress and yield. American Association for the Advancement of Sci. 206–219.

486 Stramma LS, Schmidtko LA Levin, Jonhson GC (2010) Ocean oxygen minima
487 expansions and their biological impacts. Deep-Sea Res I 57: 587–595.

488 Tang, KW, Freund, CS, Schweitzer CL (2006) Occurrence of copepod carcasses in the lower
489 Chesapeake Bay and their decomposition by ambient microbes. Estuarine, Coastal and Shelf
490 Science 68: 499–508.

491 Tang KW, Bickel SL, Dziallas C, Grossart HP (2009) Microbial activities accompanying
492 decomposition of cladoceran and copepod carcasses under different environmental conditions.
493 Aquatic Microbial Ecology 57: 89–100.

494 Tang KW, Gladyshev MI, Dubovskaya OP, Kirillin G, Grossart HP (2014) Zooplankton
495 carcasses and non-predatory mortality in freshwater and inland sea environments. J Plankton Res
496 36: 597–612.

497 Tang KW, Elliott D T (2014) Copepod carcasses: Occurrence, fate and ecological importance.
498 Copepods: Diversity, Habitat and Behaviour, Pages: 255 – 278.

499 Tang KW, Blackhaus LV, Riemann L, Koski M, Grossart H-P, Munk P, Nielsen TG (2019a)
500 Copepod carcasses in the Subtropical Convergence Zone of the Sargasso Sea: Implications for
501 microbial community composition, system metabolism and carbon flux. J Plankton Res (in
502 press).

503 Tang KW, Ivory JA, Shimode S, Nishibe Y, Takahashi K (2019b) Dead heat: Copepod carcass
504 occurrence along the Japanese coasts and implications for a warming ocean. ICES J Mar Sci (in
505 press).

506 Thiel M, Macaya EC, Acuña E, Arntz WE and others (2007) The Humboldt Current System of
507 Northern and Central Chile: oceanographic processes, ecological interactions and socioeconomic
508 feedback. Oceanogr Mar Biol Ann Rev 45: 195–344.

509 Tsuda A (1994). Starvation tolerance of a planktonic marine copepod *Pseudocalanus newmani*
510 frost. J Exp Mar Biol Ecol 181: 81–89.

511 Vargas CA, Escribano R, Poulet S (2006) Phytoplankton diversity determines time windows for
512 successful zooplankton reproductive pulses. Ecol 87: 2992–2999.

513 Wetzel RG (1995) Death, detritus, and energy flow in aquatic ecosystems. Fresh Biol 33: 83-89.

514 Yañez S, Hidalgo P, Escribano R (2012) Natural mortality of *Paracalanus indicus* (Copepoda:
515 Calanoida) in coastal upwelling areas associated with oxygen minimum zone in the Humboldt
516 current system: implications for the passive carbon flux. Rev Biol Mar Oceanogr 47: 295–310.

517 Yañez S, Hidalgo P, Ruz P, Tang K (2018) Copepod secondary production in the sea: assessing
518 errors associated with the molt rate method and incidence of carcasses. Progr Oceanogr 165:
519 257-267. https://doi.org/10.1016/j.pocean.2018.06.008.

520 Zar JH (1984) Biostatistical Analysis. Prentice-Hall International Inc., New Jersey, 718 pp.

521

522

523

524

525 Table 1: Results of Spearman rank order correlations of predatory and non-predatory mortality
526 rates (d^{-1}) with oceanographic variables: temperature (T), salinity (S), dissolved oxygen (DO)
527 and chlorophyll *a* (Chl *a*). * indicates significant correlation at $p < 0.05$.

Variable		**Predatory mortality rates**				**Non-predatory mortality rates**			
		T	**S**	**DO**	**Chl *a***	**T**	**S**	**DO**	**Chla**
Paracalanus cf. *indicus*	R	0.117	0.143	0.236	-0.099	-0.083	0.317	-0.596	-0.374
	P	0.202	0.120	0.009*	0.291	0.117	0.117	0.000*	0.000*
	n	72	72	72	72	71	71	71	71
Acartia tonsa	R	0.132	0.074	0.352	-0.226	0.022	0.065	-0.574	-0.175
	P	0.151	0.420	0.006*	0.013*	0.676	0.219	0.000*	0.001*
	n	71	71	71	71	72	72	72	72
Calanus chilensis	r	-0.290	-0.102	0.127	0.127	0.532	0.077	0.112	-0.161
	P	0.001*	0.269	0.165	0.058	0.002*	0.143	0.702	0.102
	n	69	69	69	69	71	71	71	71

528

529

530

531

Table 2. Average prosome length (μm), stage-specific total mortality rate (d^{-1}) and its partition between predatory (PM) and non-predatory (NPM) sources (%).

	Paracalanus cf. *indicus*				*Acartia tonsa*				*Calanus chilensis*			
Stage	Prosome length	Total mortality	% PM	% NPM	Prosome length	Total mortality	% PM	% NPM	Prosome length	Total mortality	% PM	% NPM
C1	350.0	0.15	53.3	46.7	528.0	0.15	60.0	40.0	940.0	0.11	63.6	36.4
C2	426.7	0.18	55.6	44.4	596.7	0.17	58.8	41.2	1126.0	0.29	69.0	31.0
C3	592.6	0.24	54.2	45.8	657.9	0.22	54.5	45.5	1278.3	0.32	68.8	31.2
C4	724.7	0.35	54.3	45.7	730.0	0.32	56.3	43.7	1491.7	0.42	66.7	33.3
C5	844.0	0.55	50.9	49.1	870.4	0.46	52.2	47.8	1812.0	0.45	57.8	42.2
		avg	*53.7*	*46.3*		*avg*	*56.4*	*43.6*		*avg*	*65.2*	*34.8*

Figure Captions

Figure 1: Upwelling zone in Mejillones Bay (23°S) where samples were collected.

Figure 2: Oceanographic conditions (average of three station samples): a) Upwelling index expressed as Ekman transport ($m^3\ s^{-1}\ km^{-1}$), b) temperature, c) salinity, d) dissolved oxygen and e) Phytoplankton biomass, measured as chlorophyll *a*, in Mejillones Bay (northern Chile) during 2010-2011. The white stripped line represents the change between years of sampling.

Figure 3: Monthly predatory mortality rates (mean ± sd) of the three major copepod species in 2010 and 2011 at Mejillones Bay. Months without data points mean the species was absent in the samples.

Figure 4: Monthly non-predatory mortality rates (mean ± sd) of the three major copepod species in 2010 and 2011 at Mejillones Bay. Months without data points mean the species was absent in the samples.

Figure 5: Total mortality rate as a function of copepodite stages for the three major copepod species in Mejillones Bay. Lines are linear regression functions fitted at $p < 0.05$.

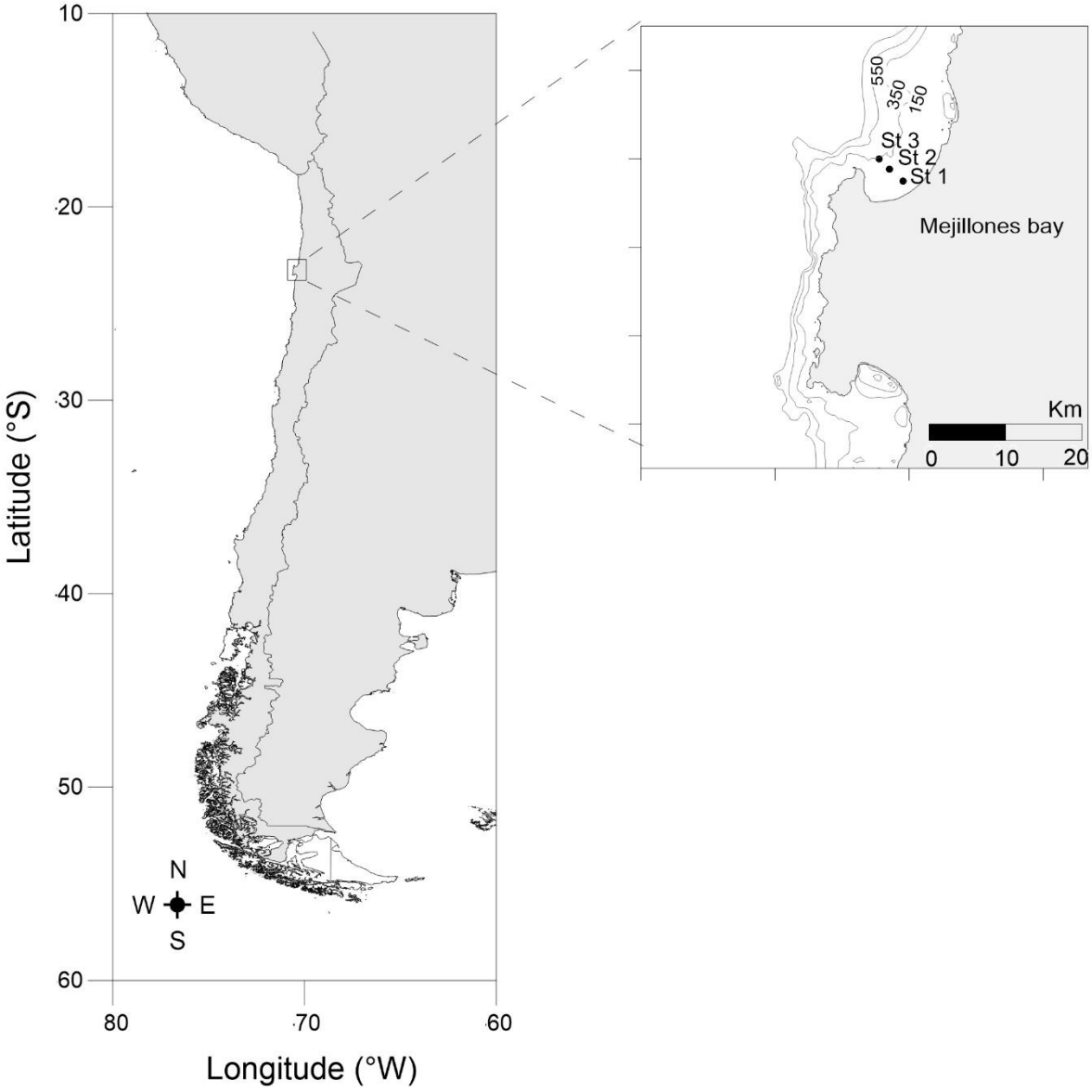
10
20
30
40
50
60
80
70
60
Latitude (°S)
Longitude (°W)
N
W
E
S
550
350
150
St 3
St 2
St 1
Mejillones bay
Km
0
10
20

Figure 1

568

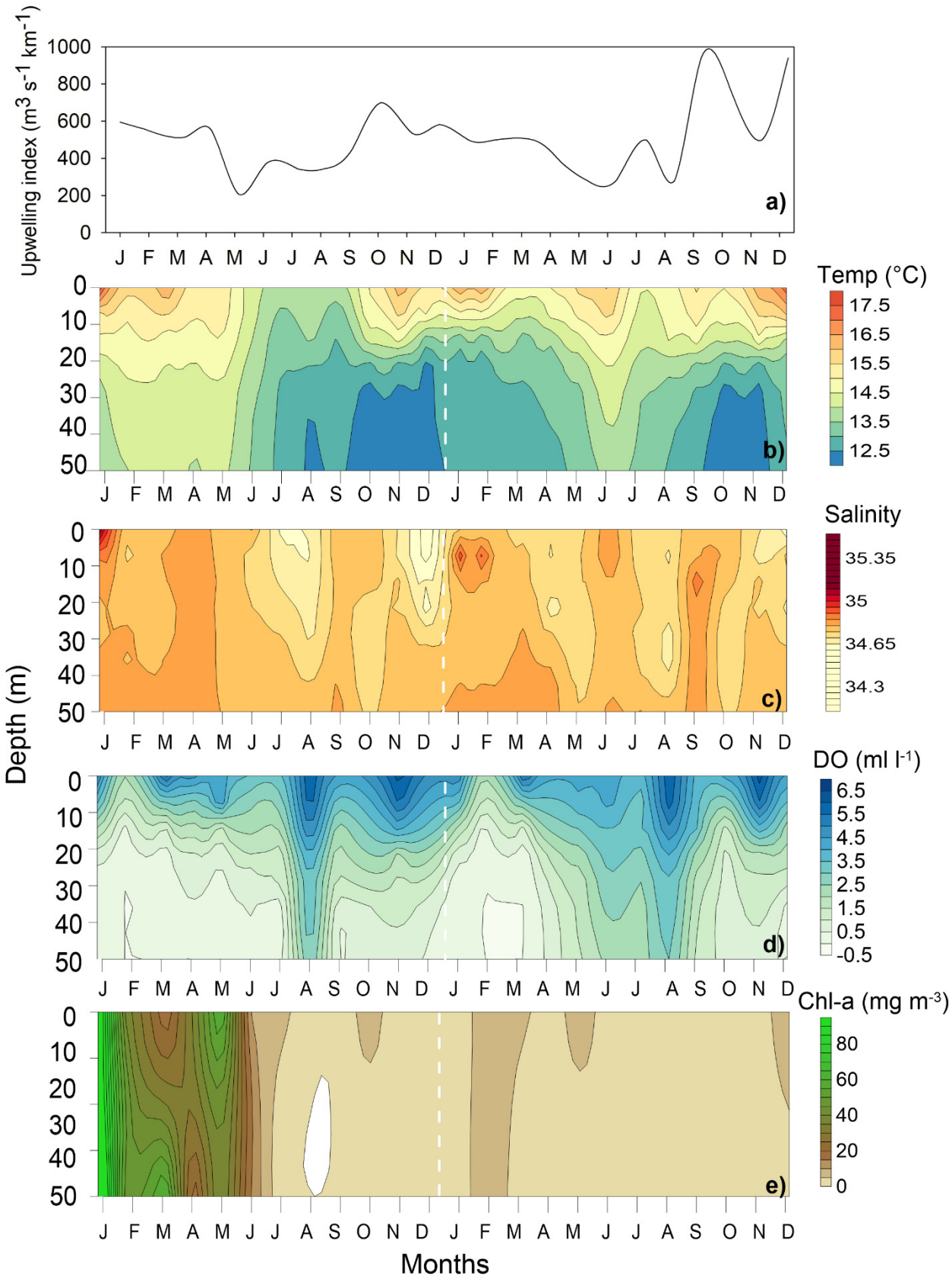

569

570 **Figure 2**

571

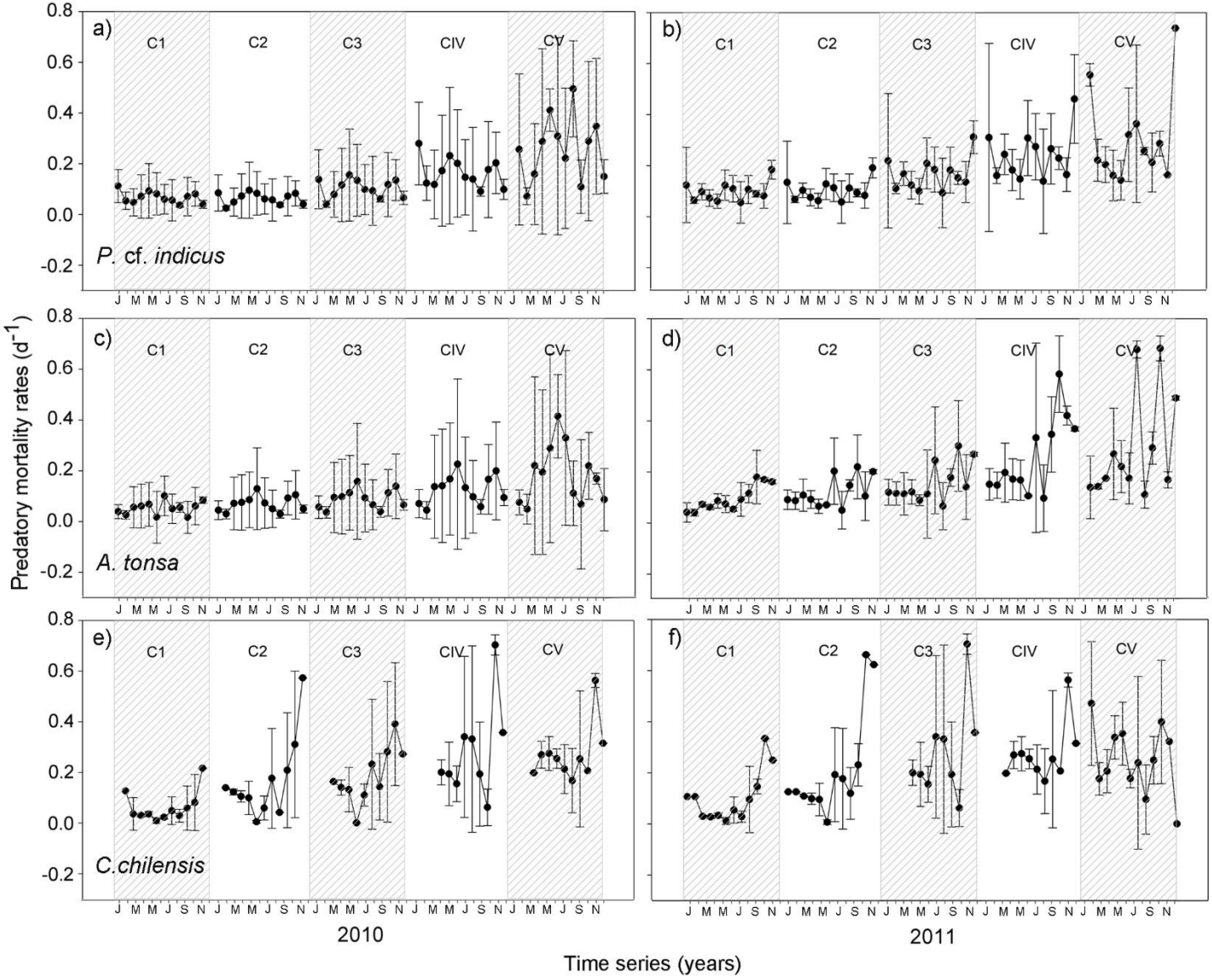
a)
b)
c)
d)
e)
f)
C1
C2
C3
CIV
CV
P. cf. indicus
A. tonsa
C.chilensis
Predatory mortality rates (d-1)
0.8
0.6
0.4
0.2
0.0
-0.2
J M M J S N J M M J S N J M M J S N J M M J S N J M M J S N
2010
2011
Time series (years)

Figure 3

589 **Figure 4**

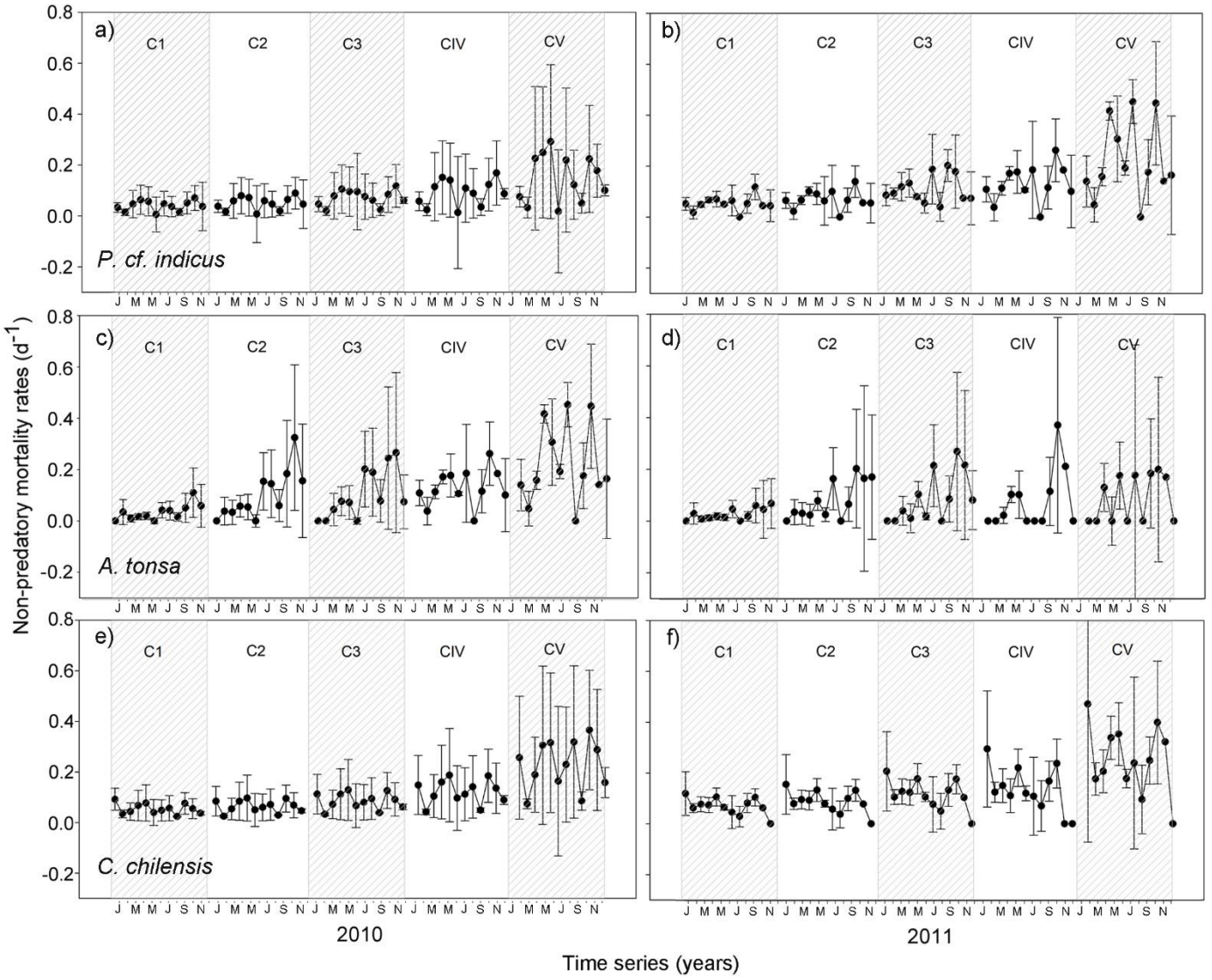
a)
b)
c)
d)
e)
f)
C1
C2
C3
CIV
CV
P. cf. indicus
A. tonsa
C. chilensis
Non-predatory mortality rates (d-1)
0.8
0.6
0.4
0.2
0.0
-0.2
J M M J S N J M M J S N J M M J S N J M M J S N J M M J S N
2010
2011
Time series (years)

590

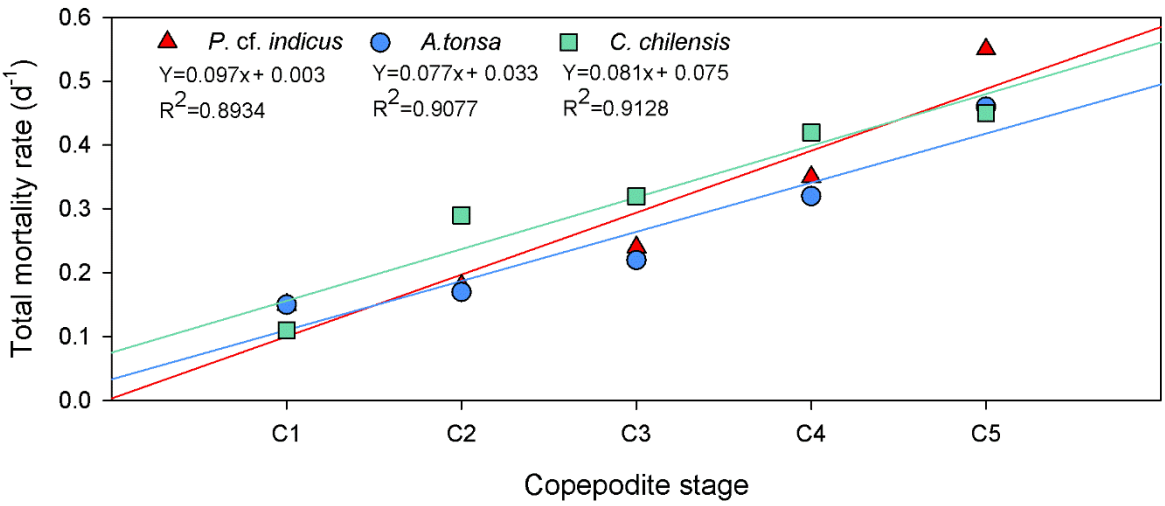

591
592
593
594 **Figure 5**
595

Table S1: Formulations and parameters for estimates stage durations, predatory and non-predatory mortality rates.

Parameter	**Symbol**	**Unit**	**Note**
Stage duration	D	Days	Stage-specific D_i is indicated by subscript i; $i+1$ for consecutive stages
Development time	a_i	Days	Stage-specific a_i is indicated by subscript i
Temperature	T	°C	Estimated from field conditions
Alpha	α	°C	Solved by nonlineal least square regression (*nls* function in R)
Beta	b	Dimensionless	
Molting rates	MR	d^{-1}	Stage-specific MR is indicated by subscript i
Number of individuals in molting rate experiment	N	Dimensionless	Consecutive stages are indicated by subscripts i and $i+1$
Time	t	h	
Abundances	A	$ind.m^{-3}$	Used for Abundances ratio in Predatory mortality rates. Consecutive stages are indicated by subscripts i and $i+1$ and adults (A_q)
Predatory mortality rates	δ	d^{-1}	Solved for iteratively
Proportions of individuals	π		π_1 y π_2 are proportions live and dead, respectively in stage i ; π_3 y π_4 are proportions live and dead, respectively in stage $i+1$
Carcasses turnover time	τ	days	
Total mortality	mt	d^{-1}	
Non-predatory mortality rates	m	d^{-1}	
Calculations of stage durations:			

Stage duration from Bèlehràdek equation (1935)	
$Di = a_i (T - \alpha)^b$	(1)
MR method (Runge et al. 1985; Kimmerer & McKinnon 1987)	
$MR = (\frac{N_i + N_{i+1}}{N_i}) \times t$	(2)
$ai=1/MR$	(3)
Calculations from non-predatory mortality	
Carcasses turnover time (Elliott et al., 2010)	
$\tau = e^{(\frac{3,83}{4,166(1-e^{-0,008T})+0,046DO}-1,39)}$	(4)
Predatory mortality rates (from VLT equations; Elliott and Tang, 2011)	
$\frac{Ai}{Ai+1} = \frac{1-\pi_1 e^{(-\delta i Di)} - \pi_2 e^{(-\delta i \tau)}}{\pi_1 e^{(-\delta i Di)}[1-\pi_3 e^{(-\delta i Di+1)} - \pi_4 e^{(-\delta i \tau)}]}$	(5)
$\frac{Ai}{Aq} = \frac{1-\pi_1 e^{(-\delta i Di)} - \pi_2 e^{(-\delta i \tau)}}{\pi_1 e^{(-\delta i Di)}[1-\pi_4 e^{(-\delta i \tau)}]}$	(6)
Total mortality rates (from VLT equations; Elliott and Tang, 2011)	
$Total\ mortality\ (mt, d^{-1}) = \mathrm{Ai} + 1\ (\frac{e^{(\delta i Di)} - 1}{1 - e^{(\delta i Di+1)}})$	(7)
Non-predatory mortality rates (Elliott and Tang, 2011; Tang and Elliott, 2014)	
Once predatory and total mortality rates had been calculated, non-predatory mortality rate is then calculated as the difference between total and predatory mortality rate: $m = mt - \delta$	(8)

Table S2: Oceanographic variables in Mejillones Bay during 2010−2011.

Variable	**2010**				**2011**			
	Mean	Max.	Min.	SD	Mean	Max.	Min.	SD
Temperature at 10 m (°C)	13.39	14.37	12.62	0.72	13.19	14.10	12.63	0.38
Temperature at 50 m (°C)	14.55	15.52	13.09	0.78	14.55	15.52	13.31	0.77
Salinity at 10 m	34.75	34.83	34.62	0.07	34.78	34.83	34.77	0.02
Salinity at 50 m	34.80	34.85	34.75	0.03	34.80	34.83	34.75	0.03
Dissolved oxygen at 10 m (mL L^{-1})	2.86	5.42	1.22	1.30	0.98	3.02	0.00	0.99
Dissolved oxygen at 50 m (mL L^{-1})	0.47	3.02	0.00	0.98	3.37	1.24	5.42	1.22
Chlorophyll *a* at 10 m [mg m^{-3}]	24.03	102.0	0.60	31.22	4.19	10.08	0.93	2.85
Chlorophyll *a* at 50 m [mg m^{-3}]	25.20	116.8	0.02	36.21	1.56	9.98	0.04	2.74

Table S3: Results of two-factor General Linear Model (GLM) for stage durations as functions of months and developmental stages. * indicates significant difference at $p < 0.05$.

Variable		**Stage duration**		
		df	**F**	***p***
P. cf. *indicus*	Months	23	2.77	0.000*
	Stages	4	1.73	0.000*
A. tonsa	Months	23	1.18	0.000*
	Stages	4	2.41	0.000*
C. chilensis	Months	23	7.45	0.000*
	Stages	4	5.78	0.000*

Table S4: Results of General Linear Model (GLM) for oceanographic variables at the coastal upwelling zone of northern Chile during 2010−2011.

Variable		**F**	***P***
Chlorophyll *a*	Seasons	2.77	< 0.05
	Years	2.74	< 0.05
Ekman transport	Seasons	4.08	< 0.05
	Years	0.28	0.626
Salinity	Seasons	2.36	0.055
	Years	0.24	0.626
Dissolved oxygen	Seasons	6.63	< 0.05
	Years	0.82	0.374

Table S6: Results of two-factor General Linear Model (GLM) for predatory and non-predatory mortality rates (d^{-1}) as functions of months and developmental stages. * indicates significant difference at $p < 0.05$. Stations were treated as replicates.

Variable		**Predatory mortality rates**			**Non- predatory mortality rates**		
		df	**F**	***p***	**df**	**F**	***P***
P. cf. *indicus*	Months	23	10.35	0.001*	23	2.18	0.140
	Stages	4	21.68	0.000*	4	18.56	0.000*
A. tonsa	Months	23	43.53	0.000*	23	5.69	0.000*
	Stages	4	42.74	0.000*	5	12.97	0.000*
C. chilensis	Months	23	11.31	0.001*	23	3.30	0.070
	Stages	4	9.82	0.000*	4	4.21	0.002*

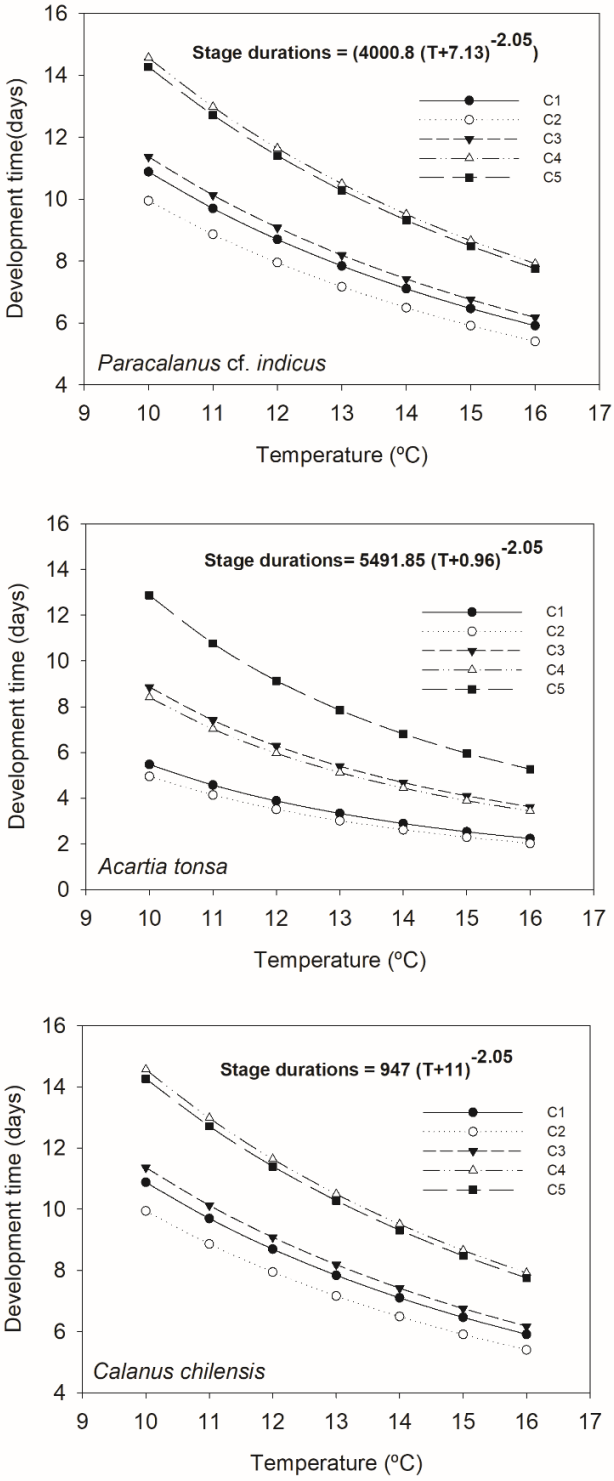

Figure S1. Copepodite stage duration for the three major copepod species as a function of temperature T (from Bèlehràdek equation) at Mejillones Bay.